Brain-Computer Interfaces

Brain Connectivity Evaluation during Sustained Attention Using EEG-based Brain-computer Interface --Manuscript Draft--

Full Title:	Brain Connectivity Evaluation during Sustained Attention Using EEG-based Brain-computer Interface	
Manuscript Number:		
Article Type:	Special Issue Article	
Keywords:	Brain-Computer Interface, Sustained attention, Granger Causality, Brain connectivity, EEG	
Manuscript Classifications:	Application development and evaluation; EEG (event-related synchronization/desynchronization); Human cognition; Signal acquisition	
Abstract:	Attention has a primary role in cognition and object selection. Sustained attention, also known as vigilance, refers to the capability of maintaining focus on a task over a prolonged period. Attentional deficits may be caused by several neurological diseases such as (ADHD), Alzheimer's disease (AD), Mild Cognitive Impairment (MCI), Traumatic Brain Injuries (TBI), Post-Traumatic Stress Disorder (PTSD), etc. The objective of this work is to evaluate sustained attention under visual stimulations of scenes and faces using an EEG-based brain-computer interface platform. The experiment consisted of two phases: image recognition and attention evaluation. During both phases, the response time to faces is significantly less than that to scenes. We analyzed event-related time-frequency representation of faces and scenes under both disturbance-free (phase 1) and disturbed (phase 2) conditions. We also investigated causal relationship between object recognition and the motor response associated with the category selection using the brain connectivity evaluated via Granger causality. The developed experimental protocols and connectivity evaluation methods may provide insights for better understanding of the neural processes for object recognition and category selection.	

Brain Connectivity Evaluation during Sustained Attention Using EEG-based Brain-computer Interface

Soheil Borhani, Reza Abiri, Yang Jiang, Taylor Berger, and Xiaopeng Zhao

Abstract— Attention has a primary role in cognition and object selection. Sustained attention, also known as vigilance, refers to the capability of maintaining focus on a task over a prolonged period. Attentional deficits may be caused by several neurological diseases such as (ADHD), Alzheimer's disease (AD), Mild Cognitive Impairment (MCI), Traumatic Brain Injuries (TBI), Post-Traumatic Stress Disorder (PTSD), etc. The objective of this work is to evaluate sustained attention under visual stimulations of scenes and faces using an EEG-based brain-computer interface platform. The experiment consisted of two phases: image recognition and attention evaluation. During both phases, the response time to faces is significantly less than that to scenes. We analyzed event-related time-frequency representation of faces and scenes under both disturbance-free (phase 1) and disturbed (phase 2) conditions. We also investigated causal relationship between object recognition and the motor response associated with the category selection using the brain connectivity evaluated via Granger causality. The developed experimental protocols and connectivity evaluation methods may provide insights for better understanding of the neural processes for object recognition and category selection.

Index Terms— Brain-Computer Interface, Sustained attention, EEG, Event-related potential, Granger Causality, Time-frequency, Brain connectivity

I. INTRODUCTION

Great advances have taken place in Brain-Computer Interface (BCI) since its initial establishment in the 1960s [1]. Brain as a complex system, contains nonlinear dynamics and nonstationary behavior, which makes it difficult to describe. Making assumptions could simplify the understanding of the brain. Recently, model-based approaches offer a systematic modelling of complex systems such as brain. The approach mitigates the curse of dimensionality by making some assumptions about the structure, dynamics, or statistics of the system under observation. By modelling, we can make some assumptions to tractably understand the system. Here, the complex system (e.g. brain model with millions of neurons) is estimated with linear dynamics and far fewer variables.

This work was in part supported by Alzheimer's Tennessee, the NIH under grants AG028383 and UL1TR000117, and the NSF under Award #1659502.

- S. Borhani is with the Department of Mechanical, Aerospace, and Biomedical Engineering, The University of Tennessee, Knoxville, TN 37996 USA (e-mail: sborhani@vols.utk.edu).
- R. Abiri is with the Dept. of Neurology at University of California, San Francisco/Berkeley and Dept. of Mechanical, Aerospace, and Biomedical Engineering at the University of Tennessee, Knoxville (e-mail: reza.abiri@ucsf.edu).

According to Bullmore and Sporns [2], there are three types of brain connectivity:

- 1) Structural (anatomical) connectivity. This type of connectivity describes how different areas of brain are anatomically wired together [3]. It shows how different parts of the brain can communicate with each other. The axial dendritic connections in the brain depicts the possibility of exchanging information and not the actual connection in every moment. Methods such as Diffusion Tensor Imaging (DTI) can visualize this kind of connectivity. This type of connectivity is state invariant; the dynamics of this connectivity at the level of networks of the brain evolves very slowly over the course of days and years [4].
- 2) Functional connectivity. Taking the assumption that different areas of brain can communicate with each other, functional connectivity studies correlation patterns and spectral coherence between different areas [5]. Although this type of connectivity is dynamic, state dependent, and can evolve in the order of milliseconds and seconds, it does not necessarily imply a causal link [6].
- 3) Effective connectivity. The method suggests that different areas of brain may have not only correlative activities but also causal relationships. One area can exchange information and drive another area. The connectivity is dynamic, state dependent, and can evolve in the order of milliseconds and seconds. While the functional connectivity can reveal mutual synchronization between different brain regions, the effective connectivity aims to uncover causal interaction and connectivity among sources of brain activities.

Here, we explored effective connectivity in a sustained attention task. We exposed a number of healthy human participants to 1) a sequence of images of faces and scenes, and 2) a sequence of superimposed face and scene images, while priming them to maintain focus, and distinguish between the image categories. The electroencephalogram (EEG) time series were collected during the tasks using a 14-channel EEG headset. We utilized the concept of Granger causality [7]

- Y. Jiang is with the Department of Behavioral Science, College of Medicine, at University of Kentucky, Lexington KY, USA (e-mail: yjiang@uky.edu).
- T. Berger is with the Department of Mechanical, Aerospace, and Biomedical Engineering, University of Tennessee, Knoxville, TN 37996 USA (e-mail: tberger3@vols.utk.edu).
- X. Zhao is with the Department of Mechanical, Aerospace, and Biomedical Engineering, University of Tennessee, Knoxville, TN 37996 USA (e-mail: xzhao9@utk.edu).

between selected sources of brain activities to reveal the interdependence between different brain regions using the EEG time-series. According to the Granger causality scheme, a time-series x(n) can be granger cause of another time-series y(n) if information about x(n)'s past improves the prediction of the variable y(n), above and beyond the information contained in past of y(n) (and other measured variables) [8, 9]. We focused on the metric of Granger-Geweke Causality (GGC) as a measure of directed connectivity [10-12].

II. MATERIALS AND METHODS

A. Participants

Thirty-eight college students (11 females: 21.3±1.9 years and 27 males: 23.1±5.2 years) participated in the experiment. There were 33 right-handed and five left-handed participants. Only right-handed participants were included in this study. They all had normal or corrected to normal vision. They had no known history of neurological or psychological disorder. The experimental protocol was approved by the Institutional Review Board at the University of Tennessee, Knoxville. All participants were asked to read and sign a consent form prior to participating in the study. The experiment consisted of two phases, which are described in Sections II.C and II.D.

B. EEG recording

EEG Data was acquired using a water-hydrated 14-channel Emotiv EPOC wireless EEG headset over AF3, F7, F3, FC5, T7, P7, O1, O2, P8, T8, FC6, F4, F8, AF4 according to 10-20 standard with a sampling rate of 128Hz. We ensured to maintain low impedance (<10K Ω) for all EEG electrodes during the experiments. The EPOC TestBench software was used to monitor the quality of EEG signals. The received signals were referenced with respect to P3/P4 electrodes over left and right mastoids.

C. Phase 1: Image recognition

1) Experimental protocol

Each participant was conditioned to recognize 200 "Face" and 200 "Scene" individual images as trials by keypresses. The conditioned trials were divided into eight blocks, in which the two image categories were equally distributed. There was a short pause between blocks. The participants were exposed to male and female faces in four blocks and indoor and outdoor scenes in the other four blocks. To ensure high attention to the image category throughout the experiment, we instructed the participants to distinguish between the subcategory images. An illustration of this phase is shown in Fig. 1. The sequence of images was displayed on a 33cm×33cm LCD monitor with a 60 Hz refresh rate and 1920×1200 resolution. Participants were asked to look at the center of the monitor and keep their distance at 60 cm. Each trial was a single greyscale image followed by a black screen. Each block started with a 1000ms cue texture that guided participants on the attended images and the expected behavioral response. Then, it continued with showing single images randomly selected from scene subcategories (Indoor scene & outdoor scene) or face subcategories (male face & female face) with a black screen between images. Each image was shown for 1000ms and the inter-trial duration was a random variable between 1000ms and 1500ms. Overall, 50 images were shown to each participant during each block.

A computer keyboard was used to collect behavioral responses of participants. Pressing Back quote button on the top left corner collected left hand responses and hyphen button on the top right corner collected right hand responses. Table I shows the expected behavioral responses for corresponding subcategories of images for eight blocks. Keyboard button assignments were counterbalanced across all blocks to minimize the projection of motor-related activities over EEG signals. A one-minute practice block was designed to familiarize the participants with the task. The participants were asked to minimize eye blinks and body movements during the experiment. This phase took approximately 20 minutes.

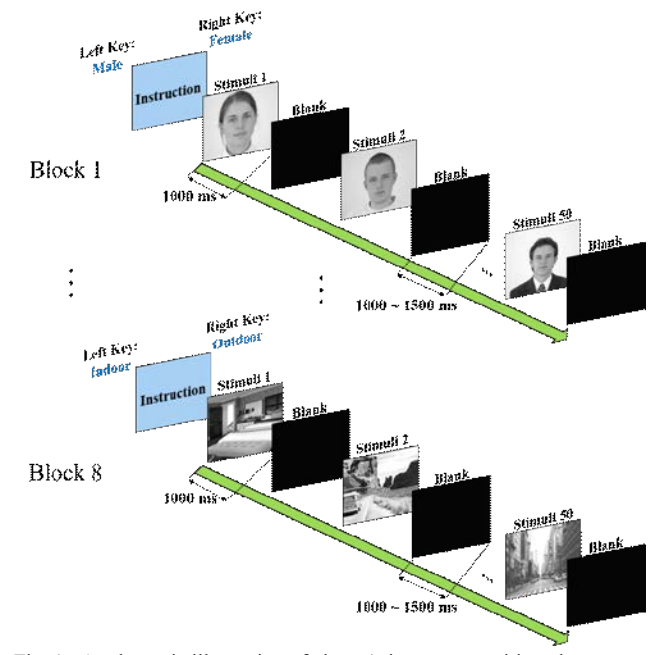


Fig. 1. A schematic illustration of phase 1: image recognition phase.

TABLE I

THE SUBCATEGORIES OF IMAGES TO WHICH A PARTICIPANT SHOULD PAY ATTENTION DURING EACH BLOCK AND THE EXPECTED BEHAVIORAL RESPONSES FROM THE PARTICIPANT.

Block No. and stimuli	Left-Hand	Right-Hand
(attended) category	Response	Response
1: Face category	Male face	Female face
2: Scene category	Indoor scene	Outdoor scence
3: Scene category	Outdoor scence	Indoor scene
4: Face category	Female face	Male face
5: Scene category	Indoor scence	Outdoor scence
6: Face category	Male face	Female face
7: Face category	Female face	Male face
8: Scene category	Outdoor scene	Indoor scence

The same sequence was maintained for phases 1 and 2.

2) Input and ground truth

We aimed to analyze and generate an individual model of visual attention. Since there were 33 participants in this study, the data have been utilized to analyze and generate 33

individual models. We chose a trial-wise training scheme, which considers EEG data of a whole trial as an input to the model. We primed participants to discriminate between male and female subcategories in four blocks and between indoor and outdoor subcategories in other four blocks by key presses. Using this strategy, we assumed that the participants have relatively high attention towards face and scene categories in the corresponding blocks. Consistently, the shown image category (regardless of the subcategories) during each trial has been chosen as the ground truth.

D. Phase 2: Attention evaluation

1) Experimental protocol

Each participant was conditioned to recognize 200 "Face" and 200 "Scene" superimposed images as trials by keypresses. During each trial, the participants were exposed to a male or a female face that was superimposed by an indoor or an outdoor scene image. The conditioned image trials were evenly divided into eight blocks. The participants were instructed to discriminate between male and female subcategories in the sequence of superimposed images in four blocks, and to discriminate between indoor and outdoor subcategories in the sequence of superimposed images in the other four blocks by key presses. The two conditioned image subcategories were equally distributed to cancel out the associated motor-related response on the EEG signals. There was a short pause between blocks. Fig. 2 illustrates a schematic of the phase. A pilot study was conducted using the same experimental protocol [13]. The same keyboard buttons as the phase 1 were assigned for collecting participants' behavioral response. The conditioned visual stimuli were displayed on the same screen as the phase 1. We ensured that images used to construct the superimposed images had the same opacity, contrast, and luminance level. This phase took approximately 10 minutes.

2) Input and ground truth

In phase 2, participants were conditioned to discriminate between male and female subcategories in four blocks and between indoor and outdoor subcategories in other four blocks by key presses when exposed with the sequence of composite images. Compared to the phase 1, phase 2 did not have a black screen between trials.

E. Signal preprocessing

The experimental setup was designed using MATLAB and Simulink software. While participants were performing the experiment, the continuous EEG signals as well as the key presses (behavioral responses) were recorded. Psychophysics toolbox extensions was incorporated to calculate response time (RT) and account for synchronous collection of behavioral response [14-16]. The EEG signals were filtered out using an intrinsic [0.16-46] Hz band-pass filter and stored on the computer. We utilized EEGLAB for EEG channels and source space processing using a pipeline outlined in Fig. 3 [17]. The EEG signals collected during each block of stimuli for each participant were merged together to yield a solitary set of independent component weights common to all conditions. The continuous data was first filtered with a 1 Hz high-pass Finite-Impulse Response (FIR) filter. The filter removed the signal drift, cope with the non-stationarity of EEG signals caused by

sweating and stabilize the subsequent Independent Component Analysis (ICA). Then, bad channels and large amplitude noise caused by muscle artifacts were identified and rejected using Artifact Subspace Reconstruction (ASR) [18]. Since the EEG signals are generated with no external source, the potentials over all EEG channels are summed up to zero at every moment. So, we re-referenced the EEG signals to the average channel values. Re-referencing is also helpful to reject external noise. To minimize the risk of bias in the referencing, the previously rejected channels were interpolated using sphering transformation [19]. To avoid confusion caused by the channel interpolation, we applied Principal Component Analysis (PCA) to keep the data full-rank.

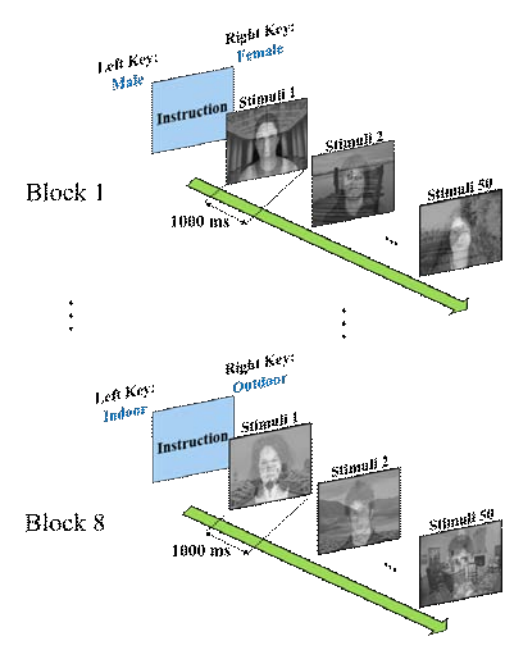


Fig. 2. A schematic illustration of phase 2: attention evaluation phase.

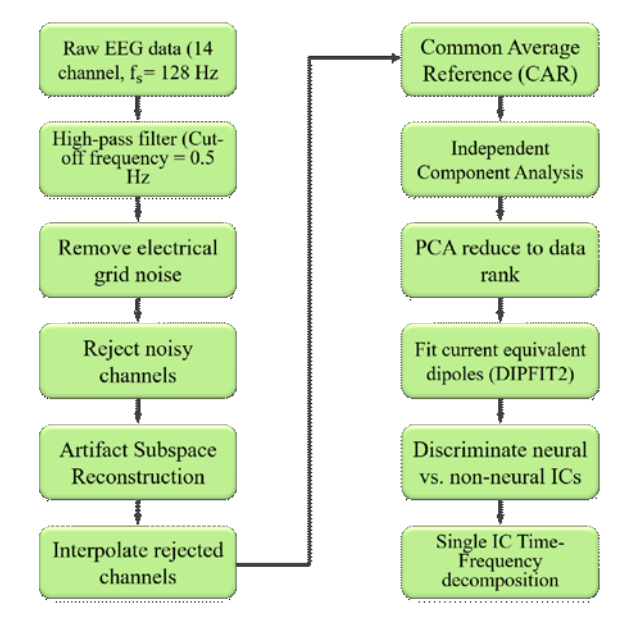


Fig. 3. Data processing pipeline using EEGLAB.

F. Independent component analysis

Brain activity measured over each EEG channel is a linear mixture of different cortical and different non-cortical sources of activities. There are methods proposed to estimate sources of activity. ICA was applied to extract maximally independent sources of information. The EEG signals recorded during all eight blocks of sustained attention task during the associated phase for each participant were combined. Then, the ICA method was applied on the continuous data to extract independent sources. The scheme yielded single set of ICA weights common to "Faces" and "Scenes" stimuli on each phase. The scheme manifests a valid approach since the EEG headset were constantly turned on and the headset placement was not altered during each phase of the experiment. This allows for comparisons of neural activity conditioned by the various visual sustained attention within spatial independent components common to the different stimuli. We used AMICA algorithm to decompose the EEG signals [19]. The algorithm pulled out the contributing source of EEG signals that helped later for signal source and causality analysis. Using Emotiv EEG headset, at most we could have extracted 14 independent sources for EEG signals collected during each sustained attention task. Each component was then projected on to the scalp map using the inverse weight matrix. We evaluated each component to discriminate between neural and non-neural signal sources using different methods. Comparing the components' activity spectrum gave a good illustration for determining the non-neural sources. With a semi-automated procedure we included mutually inclusive neural sources identified by two EEGLAB libraries named ADJUST [20] and ICLabel [21]. This allows for accurate rejection of non-neural sources. The ICA over the datasets yielded 472 ICs. We found a high commonality of more than 99% between 41 ICs of 36 participants within the right fusiform gyrus which is associated with the face fusiform form area (FFA). We focused on the participants' contributing ICs for all event-related spectral perturbation (ERSP) analysis in the result section. The data were segmented into 1200 ms epochs, starting 200 ms prior to and 1000ms after the stimulus onset. The baseline was considered the neural activity during -200 ms to 0 ms relative to stimulus onset.

G. Equivalent current dipole extraction

Following to the ICA decomposition, equivalent current dipole models were fitted for each component by using the DIPFIT2 EEGLAB extension [22]. The spherical head model was co-registered to Montreal Neurological Institute (MNI) head model to better localize the estimated current dipoles. The default parameters were applied to transform between ICA and estimated current dipole [23]. Then, Kmeans clustering was applied and estimated current dipoles were clustered into 10 different clusters. Due to the difference among participants' scalp sizes, we excluded estimated outlier current dipoles.

H. Calculation of ERSP

We focused on the estimated current dipole cluster over the FFA area (Fig. 4). Time-frequency analysis was performed using EEGLAB toolbox on all participants' ICA components on this cluster. We calculated ERSP over the epoched data to measure power fluctuations on the independent component in the frequency range of [3-40] Hz. A tapered moving Hanning

window with a Morlet wavelet transforms extracted the time-frequency event-related perturbation over all trials of each participant. We applied a linearly increasing cycle of 1 at 3Hz and 7 at 40Hz for the wavelet transform. To obtain ERSP, we averaged the spectral power across all trials of "Faces" and "Scenes" stimuli, separately. Then, the calculated spectral power converted to log power for better illustration. Baseline correction was applied by subtracting mean signal power at 100ms prior to the onset of each image category. The event-related synchronization (ERS) for both phase 1 and phase 2 has been calculated as follows:

$$ERS(freq, time) = \frac{1}{N} \sum_{i=1}^{N} |W(freq, time)|^{2}$$
 (2)

where N is the number of trials associated with a condition and W is the Morelet wavelet transform over each epoch of data. The ERSP is computed separately across trials of "Faces" and "Scenes" for each individual participant.

$$ERSP(freq, time) = 10 \log_{10} \left(\frac{ERS(freq, time)}{\Gamma} \right)$$
 (3)

where Γ is the mean spectral power at the defined baseline.

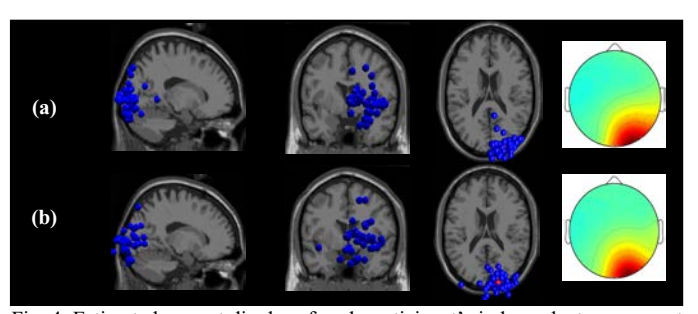


Fig. 4. Estimated current dipoles of each participant's independent component in the FFA cluster for the trials during a) "image recognition" and b) "attention evaluation" phases. The picture from left to right constitutes sagittal, coronal, and axial slices of the MNI MRI template, as well as the averaged scalp topography.

I. Group level analysis

By collecting components associated with neural patterns conditioned by faces and scenes stimuli for each individual, we conducted a group analysis using EEGLAB STUDY module. The group study allows for comparison between associated components across participants. To determine ICs with nonneural source of activities among the participants' batch datasets, we clustered all the ICs using estimated current dipoles as the feature with Kmeans clustering method into 10 clusters. Then, the time-frequency representations of neural sources in the cluster over the right occipital cortex (over the FFA) has been extracted.

J. Causal connectivity analysis

There are various post-hoc analysis applied to neural activity to estimate effective connectivity such as Dynamic Causal Modeling (DCM) [24] and structural equation modeling [25]. The methods are confirmatory in the sense that these connectivity tests can reveal connectivity by imposing different

hypothesis. By conducting statistical tests, the models can confirm if the hypothesis is significant. There are other exploratory approaches that assume a model for the neural activity and test different hypothesis under the data-driven model. We applied granger causality as an exploratory method since it is data-driven, scalable to many variables, extendable to nonlinear [26] nonstationary [27, 28] and/or nonparametric [29] systems. These characteristics makes it a good fit for EEG neural responses. The method is also capable of evaluating the hypothesis of a system being affected by an unobserved exogenous cause [30, 31]. The framework allows us to explore time and frequency varying multivariate causal relationships in the EEG data. We identified three cortical sources of interest over left occipital cortex (OccL), right occipital cortex (OccR), left supplementary motor area (SmaL), right supplementary motor area (SmaR). We assume a linear multivariate autoregressive (MVAR) dynamic system for the brain. The model describes EEG data as a linear combination of k data samples into the past. The model can represent as:

$$X_k(t) = \sum_{k=1}^{p} A_N^k(t) X_N(t-k) + E(t)$$
 (1)

where X_N is N channel EEG signals, p is the model order defined the number of data points in the past to look for causal relationship, A is the model coefficients, and E is random Gaussian noise. We assume stationarity of the data within a short time window, and stability of the model. The stability corresponds to all eigenvalues of matrix A being less than one. Practically, it means that the amplitude of the EEG as a time series is always bounded.

The important parameter to choose is the order of the MVAR model. There are different methods to determine the optimal number of data points in the past to include in the model. We can use data itself to calculate the model order. Data-driven criterion such as Akaike Information Criteria (AIC) [32], Schwarz-Bayes, and Hannan-Quinn can be utilized to calculate model order. Basically, all of these methods may suggest a different model order based on penalizing a different criterion. However, the simpler model (model with smaller p) is always preferred over other higher order models. Also, the model order depends on the EEG sampling rate. The higher the sampling rate, the higher the model order should be. Because the information above 64 Hz on the collected EEG signals may be insignificant, downsampling of the EEG signals to somewhat 100 to 120 Hz for linear modelling is preferred. Since the original sampling rate of the EEG signals (128Hz) were about the preferred sampling rate, we decided to keep the original data sampling rate. We chose the window size of 0.3 s with 90% overlap on windows to ensure the conformity with the AIC criterion [33, 34]. A range of possible model order between 1 to 40 was computed for Face and Scene trials in image recognition and attention evaluation phase for each participants' data, independently. The optimal model order for each criterion was automatically determined by choosing the minimum order that meet the constraints.

K. Connectivity model validation

In order to evaluate the accuracy of the model to capture the sources of interested dynamics, we conducted various tests. We ran whiteness test to make sure that the information left on the residuals is insignificant, consistency test with random signal as an input to the model to see if the model can generate data with the same correlation structure as the real data, and stability test to assess the stability and stationarity of the model. On average, the model order for all the participants' EEG data were 16.

III. RESULTS

A. Behavioral response

After collecting behavioral response, we examined the ability of participants to accurately distinguish between faces and scenes in both "image recognition" and "attention evaluation" phases. Specifically, we examined the difficulty of the task by evaluating the mean RT for the attended face and scene stimuli. We only included key presses during the trial and excluded all other key presses after the one-second trial. We applied a paired two-tailed t-test on the correct responses between the average RT to attended faces and scenes to determine the difficulty of focusing attention towards face versus scene for both clear and ambiguous stimuli. Fig. 5 shows the violin plot [35] of the mean correct RT for attended faces and scenes in the "image recognition" and "attention evaluation" phases. The analysis revealed a significant lower average RT for face versus scene in the "image recognition" phase (p < 0.02). This supports the assumption that, compared to scenes, it is easier to distinguish faces since faces are the most distinctive visual stimuli [36]. The question is how adding ambiguity to the visual stimuli by superimposing images with another image may affect the behavioral response. Although the t-test still shows a significant lower average RT for attended faces versus scenes (p < 0.02) on noisy images on the "attention evaluation" phase, the mean value for the two categories are very close. We also expected that adding ambiguity would increase the average RT for each attended category. The t-test also revealed a significant difference between the average RT to the attended categories between phase 1 and the ambiguous categories in the phase 2 (p < 0.02). Fig. 6 shows the percentage of correct responses in both phase 1 and phase 2. As expected, adding ambiguity to the stimuli and eliminating the inter-trial blank screen would result in lower correct responses in the "attention evaluation" phase.

B. Time-Frequency EEG response

Phase 1: Image recognition task. We inspected the corresponding time-frequency plots to identify the components of interests. Fig. 7 shows the spectral perturbation associated with face and scene stimuli conditions in one sample participant during image recognition task. Using 10% bootstrap significance level (α) on 200 trials collected under each condition for each participant's data, we filtered out the non-significant perturbations which is showed by green areas. A stronger activation pattern in frequencies (25 – 40 Hz) across scene condition compared to face condition for the image recognition phase is identified. The pattern is more pronounced within the time window between 50 and 350 ms after stimulus presentation.

Phase 2: Attention evaluation task. We also inspected the corresponding time-frequency plots to identify the components of interests. Fig. 8. depicts the calculated ERSP on a

representative participant over faces and scenes conditioned trials during attention evaluation task. The same significance level of $\alpha=10\%$ was applied to filter out non-significant perturbations. The overlapped image of face and scene seems to shift the pattern to the face conditioned stimuli. As Fig. 8 shows, a stronger activation pattern on the frequencies (15-25 Hz) for the face conditioned stimuli is depicted during attention evaluation phase. Also, scene conditioned stimuli exhibit higher gamma within the time window between 100 and 500 ms after stimulus presentation.

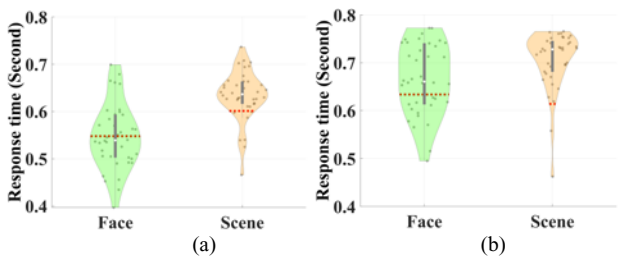


Fig. 2. Violin plot of the mean RT in the a) "Image recognition" and b) "Attention evaluation" phases. The red dotted line shows the mean correct response time (RT) over all participants.

- a) Mean[std] RT was 547[69] ms for faces and 633 [53] for scenes
- b) Mean[std] RT was 667[73] ms for faces and 706 [62] for scenes

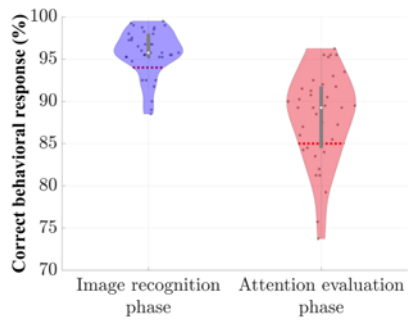


Fig. 6. Violin plot of mean correct responses in both "Image recognition" and "Attention evaluation" phases. The red dotted line shows the average over all participants. The mean[std] behavioral performance was 95.7 [2.7] % for "Image recognition" and 88.1 [5.4] % for "Attention evaluation" phases.

C. Connectivity Analysis using time-frequency distribution

We investigated causal relationships between OccL, OccR, SmaL, and SmaR brain regions for face and scene conditions. We assumed that left and right occipital areas may represent participants' perception towards attended image category while brain activities over supplementary motor area represents category selection for the behavioral task. We extracted timefrequency illustrations of granger causality between the regions of interest (ROI) considering the statistical significance of $p_value < 0.05$ for the conditioned stimuli for both "image" recognition" (Fig. 9) and "attention evaluation" (Fig. 10) phases. The figures show the changes in Granger causality over the time course of sustained attention towards different image categories between ROIs on a sample participant's data. The blue regions indicate non-significant connectivity, and the warmer regions (yellow to red) indicates stronger connectivity. During the beginning of face trials, the information outflow between the independent neural components over OccL area and SmaR area becomes hyper-coupled. The occipital region over FFA drives the neural activity in the supplementary motor

area across both Theta and Beta waves (Fig. 9.a). In contrast, the connectivity between OccL area and SmaR is more pronounced over Alpha wave (Fig. 9.b).

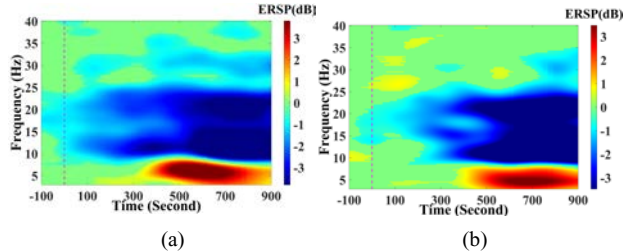


Fig. 7. ERSP response for a representative participant over all a) face and b) scene stimuli in image recognition phase

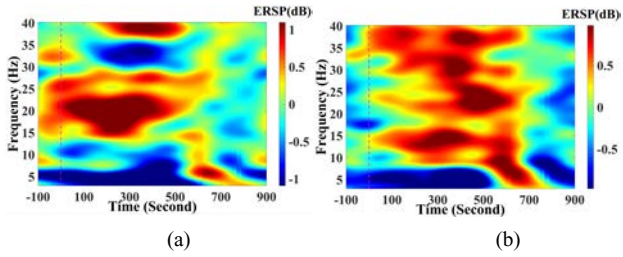


Fig. 8. ERSP response for a representative participant over all a) face and b) scene stimuli in attention evaluation phase

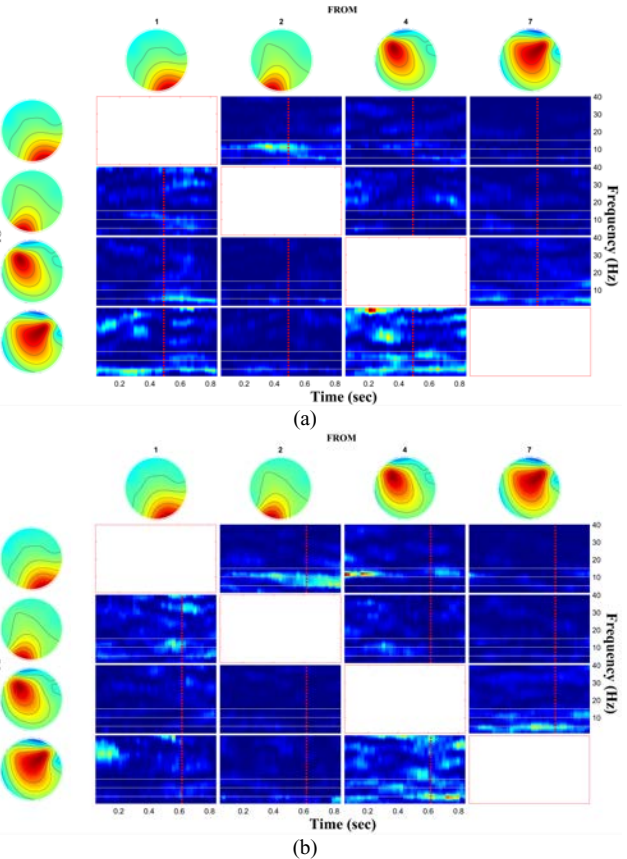


Fig. 9. Time-frequency distribution of granger causality from left occipital (OccL), right occipital (OccR), left supplementary motor area (SmaL), and right supplementary motor area (SmaR) as source on the columns to the same areas on the rows as sink for (a) Face trials and (b) Scene trials in the image recognition phase. The red dotted lines show the average behavioral response time for each condition. Non-zero connectivity with the significance level of $p_value < 0.05$ is illustrated with warm regions (Red).

IV. DISCUSSION AND CONCLUSION

In this work, we developed an EEG-based BCI platform using a portable, water-hydrated, and wireless EEG headset. We conducted a two-phase experiment to evaluate sustained visual attention to face and to scene images by exposing a group of participants to sequence of images and asking them to distinguish image categories using key presses. In the first phase, a sequence of untainted images was shown, and participants were given a pause between images. In the second phase, a sequence of noisy, superimposed images was displayed while there was no pause between trials. We analyzed stable time-frequency representations of sustained visual attention towards face and scene images both in a pure and in a noisy environment. We also investigated causal connectivity between brain regions associated with category identification and selection. Our analysis focused on the granger causality underlying sustained attention towards face and scene images in as a pure or a noisy image.

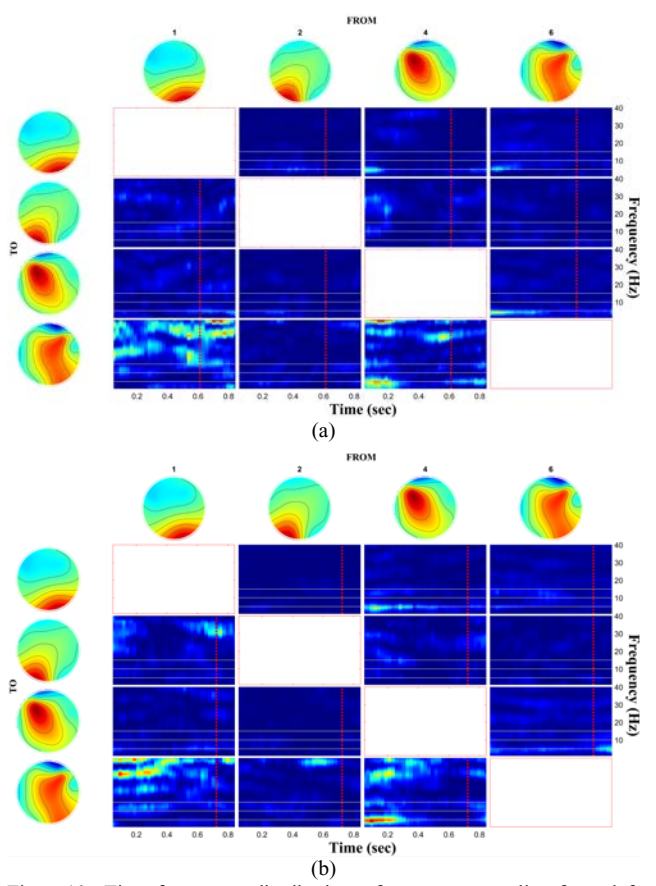


Fig. 10. Time-frequency distribution of granger causality from left occipital (OccL), right occipital (OccR), left supplementary motor area (SmaL), and right supplementary motor area (SmaR) as source on the columns to the same areas on the rows as sink for (a) Face trials and (b) Scene trials in the attention evaluation phase. The red dotted lines show the average behavioral response time for each condition. Non-zero connectivity with the significance level of $p_value < 0.05$ is illustrated with warmer regions (Red).

Connectivity models of sustained attention can provide us with a better understanding of the neural processes for object recognition and category selection. The models have been recognized and received support in the literature. Friston et al. [37] reviewed different approaches of dynamic causal

modelling. There are studies that have included measures of fMRI connectivity to predict sustained attention in people with different clinical conditions including traumatic brain injury (TBI) [38] and ADHD [39]. The measure has shown a potential to predict abnormalities in sustained attention [40] with resting state blood oxygen-level dependent (BOLD) signals. The information flow during an object-based attention has been studied with fMRI [41]. Baldauf and Desimone [41] investigated the neural connectivity during streams of overlapping objects of faces and houses. They identified the causality network between attention-related and object recognition related ROIs. The measure of EEG signals connectivity has also been investigated with resting state and task-related activities. For instance, channel-space functional connectivity using EEG signals collected in a continuous attention task were used to discriminate target and non-target visual stimuli [42]. Directionality of brain oscillations extracted with Granger causality on a visual object recognition task showed different patterns with familiar versus unfamiliar objects [43].

An interesting study for future work can be utilizing connectivity-related features in a real-time brain computer interface discrimination task. We will also conduct a group-level analysis to mathematically model the sustained attention using both neural and behavioral response to construct the model. The linear model built upon both measures may enhance our understandings of the neural structure for visual object discrimination. Moreover, future studies shall address the significance of phase-related connectivity.

V. ACKNOWLEDGMENT

We greatly thank Makoto Miyakoshi for his helpful comments on the preprocessing pipeline.

REFERENCES

- [1] L. F. Nicolas-Alonso and J. Gomez-Gil, "Brain computer interfaces, a review," Sensors, vol. 12, no. 2, pp. 1211-1279, 2012.
- [2] E. Bullmore and O. Sporns, "Complex brain networks: graph theoretical analysis of structural and functional systems," *Nature Reviews Neuroscience*, vol. 10, no. 3, p. 186, 2009.
- [3] J. P. Donoghue, "Plasticity of adult sensorimotor representations," *Current opinion in neurobiology*, vol. 5, no. 6, pp. 749-754, 1995.
- [4] R. J. Nudo, E. J. Plautz, and G. W. Milliken, "Adaptive plasticity in primate motor cortex as a consequence of behavioral experience and neuronal injury," in *Seminars in Neuroscience*, 1997, vol. 9, no. 1-2, pp. 13-23: Elsevier.
- [5] G. Nolte, O. Bai, L. Wheaton, Z. Mari, S. Vorbach, and M. Hallett, "Identifying true brain interaction from EEG data using the imaginary part of coherency," *Clinical neurophysiology*, vol. 115, no. 10, pp. 2292-2307, 2004.
- [6] A. M. Bastos and J.-M. Schoffelen, "A tutorial review of functional connectivity analysis methods and their interpretational pitfalls," *Frontiers in systems neuroscience*, vol. 9, p. 175, 2016.
- [7] C. W. Granger, "Investigating causal relations by econometric models and cross-spectral methods," *Econometrica: Journal of the Econometric Society*, pp. 424-438, 1969.
- [8] E. Siggiridou and D. Kugiumtzis, "Granger causality in multivariate time series using a time-ordered restricted vector autoregressive model," *IEEE Transactions on Signal Processing*, vol. 64, no. 7, pp. 1759-1773, 2016.
- [9] K. So, A. C. Koralek, K. Ganguly, M. C. Gastpar, and J. M. Carmena, "Assessing functional connectivity of neural ensembles using directed information," *Journal of neural engineering*, vol. 9, no. 2, p. 026004, 2012.

- [10] F. H. Lin *et al.*, "Dynamic Granger–Geweke causality modeling with application to interictal spike propagation," *Human brain mapping*, vol. 30, no. 6, pp. 1877-1886, 2009.
- [11] L. Zhang, G. Zhong, Y. Wu, M. G. Vangel, B. Jiang, and J. Kong, "Using Granger-Geweke causality model to evaluate the effective connectivity of primary motor cortex (M1), supplementary motor area (SMA) and cerebellum," *Journal of biomedical science and engineering*, vol. 3, p. 848, 2010.
- [12] M. Dhamala, H. Liang, S. L. Bressler, and M. Ding, "Granger-Geweke causality: Estimation and interpretation," *NeuroImage*, vol. 175, pp. 460-463, 2018.
- [13] R. Abiri, S. Borhani, Y. Jiang, and X. Zhao, "Decoding Attentional State to Faces and Scenes Using EEG Brainwaves," *J Complexity*, vol. 2019, 2019.
- [14] D. H. Brainard and S. Vision, "The psychophysics toolbox," *Spatial vision*, vol. 10, pp. 433-436, 1997.
- [15] D. G. Pelli, "The VideoToolbox software for visual psychophysics: Transforming numbers into movies," *Spatial vision*, vol. 10, no. 4, pp. 437-442, 1997.
- [16] M. Kleiner, D. Brainard, D. Pelli, A. Ingling, R. Murray, and C. Broussard, "What's new in Psychtoolbox-3," *Perception*, vol. 36, no. 14, p. 1, 2007.
- [17] A. Delorme and S. Makeig, "EEGLAB: an open source toolbox for analysis of single-trial EEG dynamics including independent component analysis," *Journal of neuroscience methods*, vol. 134, no. 1, pp. 9-21, 2004.
- [18] T. R. Mullen *et al.*, "Real-time neuroimaging and cognitive monitoring using wearable dry EEG," *IEEE Transactions on Biomedical Engineering*, vol. 62, no. 11, pp. 2553-2567, 2015.
- [19] A. Delorme, J. Palmer, J. Onton, R. Oostenveld, and S. Makeig, "Independent EEG sources are dipolar," *PloS one*, vol. 7, no. 2, p. e30135, 2012.
- [20] A. Mognon, J. Jovicich, L. Bruzzone, and M. Buiatti, "ADJUST: An automatic EEG artifact detector based on the joint use of spatial and temporal features," *Psychophysiology*, vol. 48, no. 2, pp. 229-240, 2011.
- [21] L. Pion-Tonachini, S. Makeig, and K. Kreutz-Delgado, "Crowd labeling latent Dirichlet allocation," *J Knowledge information* systems, vol. 53, no. 3, pp. 749-765, 2017.
- [22] R. Oostenveld, "Academic Software Applications for Electromagnetic Brain Mapping Using MEG and EEG."
- [23] C. Piazza et al., "An automated function for identifying eeg independent components representing bilateral source activity," in XIV Mediterranean Conference on Medical and Biological Engineering and Computing 2016, 2016, pp. 105-109: Springer.
- [24] K. J. Friston, L. Harrison, and W. Penny, "Dynamic causal modelling," *Neuroimage*, vol. 19, no. 4, pp. 1273-1302, 2003.
- [25] J. B. Ullman and P. M. Bentler, "Structural equation modeling," Handbook of Psychology, Second Edition, vol. 2, 2012.
- [26] W. A. Freiwald et al., "Testing non-linearity and directedness of interactions between neural groups in the macaque inferotemporal cortex," *Journal of neuroscience methods*, vol. 94, no. 1, pp. 105-119, 1999.
- [27] M. Kamiński, M. Ding, W. A. Truccolo, and S. L. Bressler, "Evaluating causal relations in neural systems: Granger causality, directed transfer function and statistical assessment of significance," *Biological cybernetics*, vol. 85, no. 2, pp. 145-157, 2001.
- [28] Y. Chen, G. Rangarajan, J. Feng, and M. Ding, "Analyzing multiple nonlinear time series with extended Granger causality," *Physics Letters A*, vol. 324, no. 1, pp. 26-35, 2004.
- [29] A. G. Nedungadi, G. Rangarajan, N. Jain, and M. Ding, "Analyzing multiple spike trains with nonparametric granger causality," *Journal* of computational neuroscience, vol. 27, no. 1, pp. 55-64, 2009.
- [30] S. Guo, A. K. Seth, K. M. Kendrick, C. Zhou, and J. Feng, "Partial Granger causality—eliminating exogenous inputs and latent variables," *Journal of neuroscience methods*, vol. 172, no. 1, pp. 79-93, 2008.
- [31] T. Ge, K. M. Kendrick, and J. Feng, "A novel extended Granger causal model approach demonstrates brain hemispheric differences during face recognition learning," *PLoS computational biology*, vol. 5, no. 11, p. e1000570, 2009.
- [32] H. Akaike, "A new look at the statistical model identification," in *Selected Papers of Hirotugu Akaike*: Springer, 1974, pp. 215-222.
- [33] H. Courellis, T. Mullen, H. Poizner, G. Cauwenberghs, and J. R. Iversen, "EEG-based quantification of cortical current density and

- dynamic causal connectivity generalized across subjects performing BCI-monitored cognitive tasks," *J Frontiers in neuroscience,* vol. 11, p. 180, 2017.
- [34] T. R. Mullen, The dynamic brain: Modeling neural dynamics and interactions from human electrophysiological recordings. University of California, San Diego, 2014.
- [35] J. L. Hintze and R. D. Nelson, "Violin plots: a box plot-density trace synergism," *The American Statistician*, vol. 52, no. 2, pp. 181-184, 1998.
- [36] B. Kaneshiro, M. P. Guimaraes, H.-S. Kim, A. M. Norcia, and P. Suppes, "A representational similarity analysis of the dynamics of object processing using single-trial EEG classification," *PloS one*, vol. 10, no. 8, p. e0135697, 2015.
- [37] K. Friston, R. Moran, and A. K. Seth, "Analysing connectivity with Granger causality and dynamic causal modelling," *Current opinion in neurobiology*, vol. 23, no. 2, pp. 172-178, 2013.
- [38] V. Bonnelle et al., "Default mode network connectivity predicts sustained attention deficits after traumatic brain injury," Journal of Neuroscience, vol. 31, no. 38, pp. 13442-13451, 2011.
- [39] M. D. Rosenberg et al., "A neuromarker of sustained attention from whole-brain functional connectivity," *Nature neuroscience*, vol. 19, no. 1, p. 165, 2016.
- [40] M. Loitfelder et al., "Abnormalities of resting state functional connectivity are related to sustained attention deficits in MS," PloS one, vol. 7, no. 8, p. e42862, 2012.
- [41] D. Baldauf and R. Desimone, "Neural mechanisms of object-based attention," *Science*, vol. 344, no. 6182, pp. 424-427, 2014.
- [42] R. Kus, K. J. Blinowska, M. Kamiñski, and A. Basiñska-Starzycka, "Transmission of information during continuous attention test," *Acta neurobiologiae experimentalis*, vol. 68, no. 1, p. 103, 2008.
- [43] G. G. Supp, A. Schlögl, N. Trujillo-Barreto, M. M. Müller, and T. Gruber, "Directed cortical information flow during human object recognition: analyzing induced EEG gamma-band responses in brain's source space," *PloS one*, vol. 2, no. 8, p. e684, 2007.